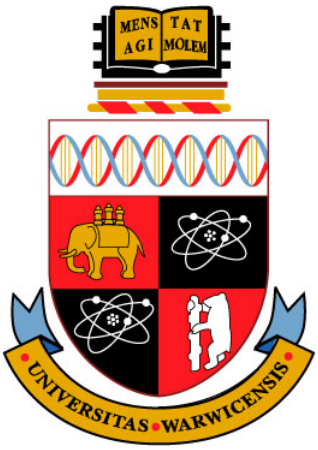

Drone-based 5G Communications Capability for Resilient Network Provision

ES327 Individual Project

Madeleine Kearns

u1921205

Supervisor: Dr. Matthew Higgins

School of Engineering

University of Warwick

Abstract

As reliance on the ability to send and receive communications over wireless networks grows globally, there is growing interest in flexible, rapidly deployable, temporary communications infrastructure with the ability to patch networks where existing ones have failed or are threatened. Potential applications of this temporary communications infrastructure are numerous, but the case for their use in disaster response and humanitarian aid is particularly compelling. Military and anti-terrorism applications are also possible.

This project aims to model a 5G wireless communications network on the University of Warwick campus, exploring its operation and how it might react to network outages. The model will use the existing infrastructure on campus. The network will be simulated in MATLAB using the 3GPP path loss model under normal working conditions, and under abnormal conditions, where a base station has been removed from the network. This will allow comparison of the two scenarios and demonstrate the significant impact on the network users that a base station being removed from the system has. The restoration of the wireless communications network capacity will then be explored, with a novel drone-based temporary communications system simulated and compared to the two previous scenarios. This will demonstrate that rapid-response drones mounted with 5G transmission antennae could re-establish reliable connectivity for the affected areas, making this a promising area of research for network resilience. In order to mimic realistic working conditions, the drone-based solution will incorporate both a higher transmission antenna and a smaller transmission power than the ground base stations, to allow for the altitude at which the drones would fly and the lower output power possible from a drone compared to a terrestrial base station.

The results from this work are novel, demonstrating that the benefits of using drones in communications include a significant reduction in shadowing and a more even distribution of received power across an area than ground base stations can achieve, with very little reduction in network capacity. Although the usage case presented here is narrow, focusing on a small geographical area, the potential applications are wide-ranging. The drone-based solution predicts a network capacity in excess of current market leaders in temporary communications systems, and relies on mature technologies, making it an exciting prospect for future research and development.

Abbreviations and Symbols

Line-of-Sight	LOS
Non Line-of-Sight	NLOS
Blocked Line-of-Sight	BLOS
Urban Micro (3GPP Propagation Scenario [1])	UMi
Suburban Macro (3GPP Propagation Scenario[1])	SMa
Unmanned Aerial Vehicle	UAV
High Altitude Platform	HAP
Transmission antenna height	h_{bs}
Effective transmission antenna height ($h_{bs} - 1.0$m)	h'_{bs}
Receiver antenna height	h_{ut}
Effective receiver antenna height ($h_{ut} - 1.0$m)	h'_{ut}
Average building height	h
Bandwidth	W
Base station transmitted power	$P_{transmitted}$
Received power	$P_{received}$
Noise	N_0
Central frequency	f_c
Distance	d
Shannon Capacity	R
Additive White Gaussian Noise	AWGN
Signal to Noise Ratio	SNR
Low Earth Orbit	LEO
Federal Communications Commission	FCC
Federal Aviation Authority	FAA
Radio Technical Commission for Aeronautics	RTCA

Contents

List of Figures

List of Tables

1 Introduction

The hypothesis of this work is that the University of Warwick campus communication system can be modelled to allow investigation into current network resilience against unexpected events. It aims to explore a novel method to improve that resilience by mounting a 5G transmission antenna onto a drone, which can then be used to replace the terrestrial base station. The project will seek to further the conversation on how this temporary emergency coverage can be provided effectively by modelling this promising potential solution and simulating how this method would perform against base station outages on the University of Warwick campus. This is expected to be directly relevant to the interests of several sectors, including (but not limited to) telecommunications companies, disaster relief and humanitarian aid, and potentially anti-terrorism and defence. The modelling will be done in MATLAB.

It is self-evident that today's communications infrastructure is vast and complex. It cannot be perfectly modelled, as it is affected so fundamentally by the world around us, which is infinitely complex and ever-changing with time and interference. Therefore, in modelling a communications system, it must be understood that only a simplified model is possible. At the same time, the reliance of modern society on digital communications cannot be overstated, and this is especially true in times of natural disaster. Telecommunications infrastructure damage leading to the affected area being denied service has become one of the hallmarks of natural disasters, as seen in the 2022 Hunga Tonga eruption and tsunami, where the loss of a single undersea fibre optic cable resulted in the entire affected area being cut off from the outside world, leaving residents unable to contact loved ones, and officials unable to coordinate an emergency response or respond to offers of help. The network remained non-operational for over five weeks [2]. Limited communication was restored using LEO satellites from SpaceX's Starlink satellite broadband program [3], but this was a slow and awkward solution, with the Starlink satellites having to first be deployed to the area, and then needing to work around geostationary satellites. It is obvious that any restoration of network capacity is better than none. It is also likely that better, faster solutions are possible, as Starlink is designed to provide broadband internet in replacement of terrestrial infrastructure, meaning that the LEO satellite constellations will be concentrated around areas that do not have terrestrial infrastructure and will need to be relocated to the affected areas.

Another potential solution to the issue of restoring communications to disaster-affected areas is the use of HAPs operating in the stratosphere to provide temporary communications networks. This route is being explored by Stratospheric Platforms Ltd, and although the results are promising in the long term, with benefits such as the HAPs being able to fly for over a week

without refuelling, and covering more ground per unit than lower-flying drones, the aerostat technology at the centre of the premise is not yet a mature technology. In the case of a natural disaster, immediate assistance is required, making it infeasible to wait for an optimal solution. Although not yet explored, it is also reasonable to assume that the time between deployment and network establishment of a HAP would be slow due to the altitude the HAP would need to ascend to. In direct contrast, drone technology is mature and widespread, with drones capable of carrying a wide variety of payloads already commercially available. Repurposing this existing technology and deploying it in response to an unfolding situation would be simple, and as drones fly at much lower altitudes than HAPs, deployment would be significantly faster. This makes drone-based solutions the most promising avenue for rapid-response temporary communications infrastructure.

Functioning networks measurably decrease the loss of life in natural disasters, with an increase in network accessibility reducing fatalities by up to 70% [4][5]. This tangible difference that being able to access the news and contact the emergency services makes to fatality rates is not the only factor making it *'vital for telecommunication companies to have [...] resources available to bring cell phone systems back online in the event of a disaster'* [5]. Providing network capacity to an area as it recovers from such an event aids the efficiency and efficacy of the response, and provides immeasurable humanitarian benefits, as those affected can contact friends and family. The exploration of using drones as a means of providing a rapid-response temporary network is therefore both of current relevance, as it is a promising alternative to the current strategies, and of great humanitarian importance. It is widely accepted that resilient communication networks have become essential to disaster response, and a robust procedure for restoring service correctly and securely in as short a time as possible will concretely reduce loss of life and human suffering.

2 Literature Review

2.1 Relevance

The network resilience of a communications network is traditionally understood as the ability of the network to maintain normal operation under abnormal conditions. Recent research into network reliability has included *availability*, or likelihood the network remains functional, and *performability*, referring to the degradation of network performance under abnormal working conditions [6]. This definition invites consideration of ways to restore networks should their functionality be reduced or removed. The 9/11 Commission Report concluded that communications failures directly contributed to the loss of at least 300 firefighters [7]. A UK Cabinet Office report into the resilience of the country's infrastructure emphasises the severity of communications losses [8]. Recent natural disasters, including the 2022 Hunga Tonga eruption and tsunami, have also demonstrated the impact that a loss of communications capability can cause. Damage to a single undersea fibre optic cable removed all communications capability, isolated $105,000$ people at a time when they needed support and aid, and severely hampered rescue and aid missions [9].

Many events may cause communications networks to run outside of their normal operating conditions, impacting the resilience of a network. The research presented in [6] provides a categorisation of these events, splitting them into categories based on cause, target, significance, and persistence. The taxonomy of network challenges presented in this paper has been used widely in further research to categorise threats to network resilience.

It has been demonstrated many times that the continued operation of a reliable and accessible communications network has a significant impact at times when there is a realistic threat to human life. Toya and Skidmore have written several articles emphasising the effect that access to a functioning communications network can have on mortality rates during natural disasters, finding that the fatality rate in unexpected natural disasters was reduced by almost 70% [4][5]. Evidently, assessing and enhancing the resilience of communications networks under disaster conditions as well as under normal operating conditions is of the utmost importance.

2.2 Justification

The current methods used to restore communications capability when a network is not operating under normal conditions are inefficient and often impractical. Mounting a satellite communications cell onto a vehicle which may be parked in the affected area (satellite trucks) is viewed as a relatively novel method of bypassing damaged terrestrial infrastructure and is employed by

the UK [10] and USA [11] emergency services. This approach is hampered by the decreased efficacy of ground-to-ground communications systems, providing network to a very small area and suffering severe losses due to the large amount of multi-path dispersion and shadowing caused by the transmission antennae being so low - on the same level as the reception antennae and therefore among the buildings and streets. Furthermore, in the aftermath of natural disasters, roads are often impassable or access to areas restricted, affecting the positioning of the satellite cell. Telecommunications companies have historically experimented with attaching transmission antennae to aerostats tethered by power and fibre lines, improving on the losses experienced by satellite trucks but introducing difficulties surrounding the safety and protection of the tethering cables, which could be dangerous in their own right and could also be sabotaged in the case of malicious human activity. The SpaceX Starlink response to the 2022 Hunga Tonga eruption and tsunami demonstrated the pitfalls of using LEO satellites for disaster relief, with the response being very delayed and employing awkward workarounds with geostationary satellites [3]. A new method to restore network operability is clearly needed.

In response to the need to explore novel ways of restoring communications without the pitfalls of the satellite trucks or aerostat approach, Saif, Dimyati *et al.* proposed the use of UAVs to provide reliable network connectivity and found performance to be 'promising' [12]. UAVs used as wireless relays between users and undamaged terrestrial infrastructure increase the possibility of LOS links, and have been shown to be effective in improving coverage [13][14]. The benefits that the flexibility and 3D capability UAVs provide in disaster scenarios is further stressed in [15] and [16], which mention the relevance of their rapid response time and that they can be deployed during a disaster rather than needing to wait for the situation to stabilise. This is echoed by Zhan, Hu, *et al.* who found drones were capable of providing high-quality emergency communications capabilities, including supporting high-resolution multi-user video streaming [14].

In considering other avenues of exploration, HAPs in the form of unmanned and untethered aerostats have also been suggested as a solution, although Grace and Mohorcic note that this technology is not yet mature [17], unlike UAVs which are widely already used for other purposes. This is reinforced by the recent experiment run by Stratospheric Platforms Ltd and the Saudi Arabian digital regulator CITC, which demonstrated the great promise of temporary infrastructure for delivering communications networks to previously disconnected areas by streaming video at 4K resolution to retail smartphones via a temporary communications network [18], but simultaneously showed that the technology for HAPs is not yet functional, as the experiment had to be conducted using a long-endurance fixed-wing aircraft rather than the targeted aero-

stat technology [19]. This makes UAV technology both more accessible and reliable. For these reasons, this project will focus on UAV approaches to restoring network capability.

2.3 Model Selection

There are three main categories of communication network models: empirical models, which are based on observations about the environment and measurements, deterministic models, which require a 3D map of the environment in order to compute the path loss specific to the scenario, and stochastic models, which require no information or assumptions about the environment and model it as a series of random variables [20]. The different models provide different predictions for the path loss of a network due to the assumptions they make about the environment and the level of detail that they have. As a 3D map of the environment was unavailable, this project could not use a deterministic model. As the environment is a familiar one, and processing power did not need to be kept at an absolute minimum, empirical models were selected over stochastic models due to their increased accuracy [21].

Currently, the most widely utilised empirical models for cellular communications are the Okumura-Hata Model, the COST231-Hata Model, and the 3GPP Path Loss Model [22]. Nkordeh, Atayero, *et al.* analyse the first two, and conclude that the COST231-Hata model reduces path loss more in urban environments, and note the benefits of elevating the antenna [23], which would be improved through the use of drones. Comparisons between close-in reference (CIR) path loss models and alpha/beta/gamma (ABG) path loss models also exist, with Thomas, Rybakowski, *et al.* concluding that the CIR model is *'more robust and reliable'* due to its physical anchor point compared to the ABG model's curve fitting base [24]. MacCartney, Zhang, *et al.* improve further on this by relying on a linear regression path loss model which improves on shadow factors compared to CIR models [25]. Despite the strengths of these models, however, the release by 3GPP of technical specifications with standard path loss models overshadow their usage. 3GPP, or the 3rd Generation Partnership Project, is a consortium of standards organisations tasked with the creation of protocols for telecommunications, shaping the mobile ecosystem. For a project with eventual practical applications, therefore, it is the obvious model to use. WMG provide documentation for the 3GPP Release 9 Path Loss Model [1]. Numerous releases have occurred since Release 9, but their additional functionality is irrelevant to this project.

An initial model for drone-to-ground LOS probability (ie, the likelihood that a drone and handheld device establish a communications link without the need for multi-path propagation) was developed by Feng *et al.* which discusses the angle of elevation of the drone in question,

allowing the optimal height for the drone to be assessed [26]. However, they did not consider the effects of shadowing on the path loss. This work was then furthered to include BLOS and NLOS situations, focusing on urban environments [27]. The minimum number of drones necessary to efficiently and reliably cover a given area is calculated in [28], along with the optimal altitude for the drones to fly at based on the coverage requirements of the area. This is outside the scope of this project, as the area under consideration is the University of Warwick campus, which is small enough that one drone is sufficient to restore coverage. However, in a larger area, multiple drones would become necessary. It has been proposed by Almalki and Angelides that a machine learning approach towards evolving the ground-to-air propagation of the network would improve the resilience and scalability of the network [29], which would be a promising extension of this work when it is scaled to needing multiple drone-mounted transmission antennae.

2.4 5G Rollout Issues

The roll out of 5G technology globally is a major step in the evolution of mobile telecommunications and marks another step down the road towards a more connected, technologically advanced society. This made the difficulties faced by the USA in turning on their 5G towers interesting. There was concern that 5G towers would cause problems with radio altimeters [30] at low altitudes. As drone-based transmission antennae would necessarily operate at low altitude, this is relevant. This concern was limited to the USA, while other countries rolled out 5G technology uninterrupted, largely due to the USA allocating 5G spectrum closer to the operating frequency of radio altimeters in the C-band than other countries. The FCC stated that well-designed equipment should not ordinarily receive any significant interference (let alone harmful interference) due to the low altitude at which altimeters are used [31]. The FCC released notice of the C-band reallocation in 2017 [32] (which included a 220Mbps protected band, included after feedback from aviation groups [33]).

Many of the concerns stem from a flawed study by the RTCA, which concluded that there was a *'major risk'* that *'harmful interference to radar altimeters on all types of civil aircraft'* would result in from the rollout of 5G [34]. This study has been largely discounted by real-world proof of a lack of significant interference from multiple countries. The RTCA study was overly conservative in both the scenarios it modelled and the criteria it applied to the altimeters tested, which were more stringent than the FAA minimum performance standards and the manufacturer design tolerance for most of the altimeters studied [33]. All Boeing and Airbus models have now been cleared by the FAA as safe from interference [35], suggesting that any issues are confined to few enough models of altimeter that the use of drone-based 5G antennae in a disaster scenario

would not impede aviation in the area due to interference. For additional precautions, instead of multi-directional transmission antennae, the drone-mounted transmission antennae could be angled down, which would limit any potential interference.

3 Modelling and Theory

3.1 Modelling the campus communications network

Modelling the campus network involved three main components – transmission, path loss, and reception of the signal. Transmission happens from one of 8 base stations on the University of Warwick campus. These are located on top of buildings. Path loss refers to the reduction in power density of the signal over a certain distance, and is caused by factors such as shadowing and multi-path dispersion. Path loss was calculated using the 3GPP Release 9 path loss models [1]. The attenuation in decibels of the signal between the transmission and reception antennae could be combined with knowledge of the strength of the transmitted signal to find the received power. This was then compared to the Shannon Capacity of the channel, in order to determine how close to the theoretical capacity limit the channel has come.

The terrestrial base stations on the University of Warwick campus were modelled as operating with a transmission power of 100mW, which is equal to 20dBm. Although on the lower end of the spectrum of the possible transmitting powers of 5G base stations, this value was chosen due to early potential of being able to conduct experiments on a similar transmission antenna. The value is therefore somewhat arbitrary and could be changed to model a network with different transmitted power very easily without noticing a significant change in the overall network behaviour. In order to create a channel model, the propagation scenario is selected, and then the network layout and antenna configuration are detailed. This project only explored path loss, which is one of three terrestrial propagation effects. Further work could investigate modelling the slow signal variation (due to shadowing and scattering) and the rapid signal variation (due to multi-path effects). The choice of parameters for the path loss models was informed by observations around campus, as well as background research into 'ballpark' figures, in order to arrive at reasonable estimates. The parameters used are listed in Table 1.

Parameter	**Symbol**	**Value**
Transmitter antenna height	h_{bs}	15m
Receiver antenna height	h_{ut}	1.2m
Average building height	h	15m
Bandwidth	W	100MHz
Base station transmitted power	$P_{transmitted}$	100mW/20dBm
Noise power	N_0	$631\text{pW}/-92\text{dBm}$
Central frequency	f_c	3.85GHz

Table 1: Modelling Parameters

The channel bandwidth used for this model was based on an analysis of the UK 5G spectrum holdings. 5G is now offered by all 4 major telecommunications companies in the UK, although it

is not yet available country-wide. The average bandwidth allocated to each network was 117MHz [36], mostly in the $3.6-4$Ghz band. This is the UK's combined coverage and capacity 5G band, balancing widespread coverage capacity and high-speed connections. A central frequency of 3.85Ghz is therefore well-positioned within this band and provides a realistic model of a 5G network on the University of Warwick campus.

The 3GPP documentation provides LOS and NLOS models. If a signal is received through a NLOS channel it will have a larger attenuation than one received through a LOS channel, due to additional multipath dispersion and absorption. 3GPP suggests several propagation scenarios, ranging from models appropriate in inner-city environments to models suited to rural applications. The University of Warwick campus is a diverse space. Therefore, to model the network across campus as realistically as possible, campus was split into three homogeneous areas. This split divides the central campus area (involving several large student accommodation blocks, the Students' Union, most campus retail centres, most social gathering points, and a high density of buildings) from the rest of campus, where the population is less dense and the buildings tend to be more spread out. Sector 1 (central campus) was assigned to the Urban Micro (UMi) propagation scenario, while Sectors 2 (Cryfield and Bluebell accommodations) and 3 (the rest of campus, including WMG and the teaching spaces) were assigned to the Suburban Macro (SMa) propagation scenario. Sector 1 has an estimated population density greater than that of central London, in large due to several large student accommodation blocks occupying a relatively small space. Furthermore, in Sector 1, buildings are relatively close together, and the area is often crowded due to the concentration of retail outlets, social spaces, and other gathering points. Sectors 2 and 3 have a far more transient population, with fewer student accommodations and more teaching spaces. While there are many people passing through the area, they are spread over a much larger area. Additionally, there is more open space in these areas, such as the Cryfield Pitches and Tocil Wood.

This analysis deliberately leaves out the satellite Gibbet Hill campus, as it has its own base station, and is far enough away from central campus that at the modelled transmission power, there is little interaction between the network on central campus and on Gibbet Hill. Further work could include this base station and examine how an outage on central campus would affect the network capacity between the two sites.

Table 2 shows the 3GPP path loss models used for each sector of campus. The minimum distance for these models to be applicable is 10m from the transmission antenna.

Sector	Propagation Scenario	3GPP Path Loss Model [1]
1	UMi	$PL = 40log_{10}(d) + 7.8 - 18log_{10}(h_{bs}^{'}) - 18log_{10}(h_{ut}^{'}) + 2log_{10}(f_c))$
2	SMa	$PL = 20log_{10}(\frac{40\pi f_c}{3}) + min(0.03h^{1.72}, 10)log_{10}(d) - min(0.044h^{1.72}, 14.77) + 0.002dlog_{10}(h)$
3	SMa	$PL = 20log_{10}(\frac{40\pi f_c}{3}) + min(0.03h^{1.72}, 10)log_{10}(d) - min(0.044h^{1.72}, 14.77) + 0.002dlog_{10}(h)$

Table 2: Path Loss Equations for the propagation scenarios used

To generate the distances for each of these models, a MATLAB script generated a large number of random coordinates within the three sectors of campus, found the nearest base station to each of the points and calculated the distance between the points and the nearest base stations. This calculation took into account the latitude, longitude, and elevation of both the transmission and reception antennae, to calculate the LOS distance using the formula below. This method allowed the users closest to each of the base stations to be isolated from each other, enabling a more granular analysis. On a much larger scale, in cases where the curvature of the Earth may prevent there being a direct LOS link, the bending of the transmission beam through the atmosphere would have to be taken into account, but on the University of Warwick campus it was not necessary for this to be a consideration.

$$d_{1,2} = \sqrt{(x_1 - x_2)^2 + (y_1 - y_2)^2 + (z_1 - z_2)^2} \tag{3.1}$$

This allowed an accurate range of distances for campus to be generated, as the modelling is focused on the network on campus and not how the base stations on campus affect the network in neighbouring areas. Using this range of distances and the parameters listed in Table 1, the path loss in decibels could be modelled for each sector. This provided the attenuation of a transmitted signal as a logarithmic ratio of the transmitted and received power. This path loss was contrasted with the free space path loss. Free space path loss disregards features such as terrain or buildings, assuming a direct LOS channel over flat ground between the transmission and reception antennae. Equation 3.2 was used to find the received power in decibel-milliwatts (dBm), an electrical power unit in decibels referenced to 1mW.

$$P_{received}[\text{dBm}] = P_{transmitted}[\text{dBm}] - PathLoss[\text{dB}] \tag{3.2}$$

Finally, the Shannon capacity of the channel was found. This is a theoretical maximum capacity, measured in bits per second (bps) that can be sent through the channel. It represents the maximum possible rate of reliable communication, or the maximum rate of communication where the error probability is arbitrarily small [37]. Approaching this theoretical band is the mark of an efficient communication channel. In order to allow high-definition video streaming, the ideal channel capacity is around 1Gbps, so this was used as the target mid-range capacity

of the channel. In order to analyse the performance of the campus network in this project, the performance was measured by the capacity and split into four levels. The target capacity was above 1Gbps. A capacity of above 800Mbps was deemed good, as this is likely to cause very minor degradation in the experience of someone using the network. Any capacity between 800Mbps and 200Mbps acceptable. Finally, capacities below 200Mbps were deemed failure. It should be noted that current development projects view a network capacity of 90Mbps as *'fantastic'* [18], with 200Mbps viewed as exceptional service [38] so this is setting a very high bar for the performance of the model.

$$R[bps] = Wlog(1 + \frac{P_{signal}}{P_{noise}}) = Wlog(1 + \frac{P_{signal}}{WN_0}) \tag{3.3}$$

To find the Shannon capacity of the channel, the signal-to-noise ratio (SNR) of the channel had to be found. This is a function of the transmitted power and the attenuation of the channel, comparing the meaningful input (P_{signal}) to unwanted input (P_{noise}). It is usually represented as a decibel value, as it is a ratio of two powers.

$$SNR_{dB} = 10log_{10}\frac{P_{signal}}{P_{noise}} = 10log_{10}\frac{P_{signal}}{WN_0} \tag{3.4}$$

For this model, Additive Gaussian White Noise (AWGN) was used. AWGN is a random process that is additive to the communications signal, and which follows a Gaussian distribution, meaning the probability distribution is symmetric about a mean value. Graphically, this appears as an unbiased bell curve. Noise is white if the power spectral density function of the process is constant, or if the noise variable is independent between samples [39]. AWGM is a good method of imitating the large number of random processes communications signals are subjected to and adding their effect to a model, increasing the accuracy when compared to a model where noise is not accounted for. These processes include shadowing, multi-path fading, and inter-symbol interference, although there are a near-infinite number of elements which might influence the communication signal. The central limit theorem, stating that the sum of independent random variables may be approximated by a Gaussian random variable, validates the choice of this method of modelling the system noise [40]. As no empirical measurements of the noise power on campus were taken, it was estimated to be -92dBm. Equation 3.5 demonstrates the model of AWGN, showing that the received value $y(k)$ is the sum of the noise-free component $y_0(k)$ and the noise component $w(k)$.

$$y(k) = y_0(k) + w(k) \tag{3.5}$$

By combining the SNR with the bandwidth as assigned in Table 1, the Shannon capacity can be found. This provides a good analysis of the modelled system, showing the maximum data rate possible under the modelled conditions. Uninterrupted high-definition video streaming capability from multiple devices is desired, so a mid-range capacity of 1Gbps is the target capacity.

To visualise the campus network, the MATLAB `coverage()`command computes a coverage map, defining received signal strength by coloured contours. This visualises shadowing and attenuation better than the received power and capacity graphs, but does not follow the 3GPP models, instead using the deterministic Longley-Rice propagation model. This is a radio propagation model suited to irregular terrain, which is somewhat limited by the approximation techniques that it uses [41] and is especially constrained in undulating terrain, when shadowing is expected to have a large effect, or over short distances [42]. While 3GPP was used for this project, the visualisation of the Longley-Rice path loss model illustrates the factors affecting the propagation of the signal and the received signal strength well.

3.2 Modelling a drone-based scenario to outage scenarios

While this report focuses on outages due to natural causes, for example terrestrial and meteorological events such as earthquakes and tsunamis, the response to a network outage is broadly applicable. The approach described in this section would be easy to adapt to a case where a temporary surge in demand for network capacity threatens to cause denial of service, such as when the usual infrastructure is ill-equipped to cope with the increased demand. This might be the case at large sporting fixtures or protests, where a larger than normal number of people are trying to access the network in a very confined space. The approach used in this report for dealing with an outage of terrestrial communications infrastructure relies on the deployment of a single axisymmetric quadcopter drone to the coordinates of the failed base station. This is sufficient for the case study of the University of Warwick campus, which is a compact area with plentiful ground communications infrastructure. The outage of a base station will have a meaningful but not catastrophic impact on the accessibility of the network, and only the network on campus is being considered, rather than the wider area which may also receive signal from the campus base stations. To scale this response to larger areas affected by natural disaster, more drones would be introduced. For this report, it is assumed that the drones have a transmission capability of 10% of the usual base station.

To showcase the effect a base station outage would have on the network availability, a base station inside Sector 1 was selected. This high-traffic area is has a large population trying to

access the network at all times, as would be the case in a natural disaster scenario. Therefore any significant drop in the network capacity may lead to denial of service to some users. The base station selected is located on top of the Student Union building, and a failure of its transmission antennae was modelled through removing it from the coverage analysis run in 3.1. As the model determines the distance between a user and all of the base stations included in the model before determining which base station they access the network through, the simple removal of a base station from the model causes users who would have been closest to this base station to be further from a transmission antenna. This results in less received power and a lower capacity at these locations. The previous analysis does not show which users are closest to which base stations, only how far they are from the nearest base station. Removing a base station will change this distribution but not the path loss model, as path loss is independent of number of users.

Therefore, to demonstrate accurately the effect the failure of a base station would have on the users who would otherwise have had it as their point of access to the network, the users who are closest to this base station are identified before the path loss is calculated. This is done by identifying users based on the index of the base station that they are closest to, and allocating those with the index corresponding to the Student Union base station to a separate set of locations. It is assumed that the users at these locations will receive their signal from the drone when it is implemented. The distances between these users and the failed base station is calculated, and only then are these distances passed to two new path loss models – one for the base station, and one for the replacement drone. This allows the direct comparison of the two transmission conditions.

The output power of a drone is largely dependent on the model of drone used. The market contains huge variation in power, size, pricing, and reliability. The range covers drones capable of carrying a modified satellite cell, which may be capable of providing as much transmission power as a terrestrial base station, to hand-held drones with very small transmission capability. An analysis of the suitability and applicability of different models of drones to this scenario is beyond the scope of this project, and would be highly tailored to each individual situation; the drone appropriate for use on the University of Warwick campus would not be the same size, power, or price as a drone appropriate for use in restoring communications to an isolated area such as Tonga in the event of a natural disaster. Therefore, the drone transmission power was set to 10% of the terrestrial base station transmission power. This allows for some scalability in the model. It is reasonable to assume that if a more powerful base station is damaged, a more powerful drone would be deployed to replace it. This is especially true as the transmitted powers

used in this analysis are low compared to commercial base stations. The relationship between the terrestrial capability and the emergency response is realistic. A private organisation such as a university would be willing to pay less for a drone replacement to cover its campus than a country at risk of natural disasters, as the stakes are far higher for the latter.

As this analysis involves one drone, the location is assumed to be the same as the terrestrial base station, as this provides the best way of comparing the network conditions under the two scenarios. Therefore, optimising the location of the drone was not necessary. However, the height of the drone was considered. Although drones are capable of lower transmission powers than terrestrial base stations, they have the advantage of transmitting from higher altitudes than terrestrial antennae, which are limited to the height of the buildings they are placed on. A higher altitude results in a wider range with lower shadowing, which is impactful in urban environments where shadowing is a major component in the path loss of a signal. However, flying the drone too high above the terrestrial antenna would cause unnecessary power to be lost as the distance between the transmission and reception antennae would dominate the received power. A drone height of 2m above the base station antenna was a reasonable compromise between the two. This additional height reduced the effect of shadowing in an urban environment significantly, due to the higher angle of incidence of the signal. This allowed the drone path loss to be modelled as suburban rather than urban, as the main factor separating the two propagation conditions is the very high effect that shadowing has in urban environments.

In order to visualise the difference that a drone transmission made compared to the usual terrestrial infrastructure, the capacity and received power of the users closest to the Student Union base station were plotted on the same axis for both scenarios. Through this direct comparison, the difference in both the capacity and received power between the drone and terrestrial base station were visualised.

If the area affected by the loss of a terrestrial base station was large enough that one drone is not sufficient to restore coverage, this approach would be adjusted. Manually positioning the drones would be possible, but there is also plentiful research and models on the best drone positioning for maximum coverage. Implementing a drone positioning software would make sense as soon as the number of drones required begins to increase. This would allow the drones to use machine learning to adjust their position autonomously. To build further resilience into the model, it would also be possible to build in redundancy, adding more drones than strictly necessary. The risk of having too many versus too few drones is not equal – too many may lead to redundancy and an unnecessary increase in costs, but too few could realistically lead to avoidable loss of life in disaster scenarios. Therefore, added redundancy would be appropriate

both in the case of natural disasters, where drones may be blown off course or damaged by debris, or in the case of malicious human activity, where drones may be intentionally damaged or shot down. These extra drones could be positioned in many ways, but the strategies generally split in two – having a constant altitude, with extra drones saturating a single layer, or having two or more different layers of drones at different altitudes, aiming to maximise both capacity and coverage by exploiting shorter transmission distances and higher angles of incidence to reduce shadowing.

4 Results

4.1 Coverage Heatmaps

The heatmaps shown in this section were calculated for the different scenarios through the MATLAB `coverage(txs)` command, which uses a Longley-Rice propagation model to calculate the coverage over a given terrain map, accounting for shadowing and multi-path dispersion. A notable exception is the free-space heatmap in Figure 4.3, which uses a free space model which does not account for terrain or buildings, but simply calculates the attenuation due to the distance between the transmitter and receiver. As `siteviewer` does not open as an image but as an object, a reduced level of image manipulation is possible. Figure 4.1 shows the received power scale used in all of the heatmaps below in higher definition.

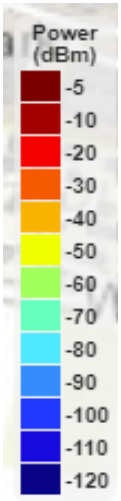

Figure 4.1: Enlarged view of the received power gradient scale used in all coverage heatmaps hereafter. The conversion between decibel-milliwatts (dBm) and Watts is discussed in the Modelling chapter.

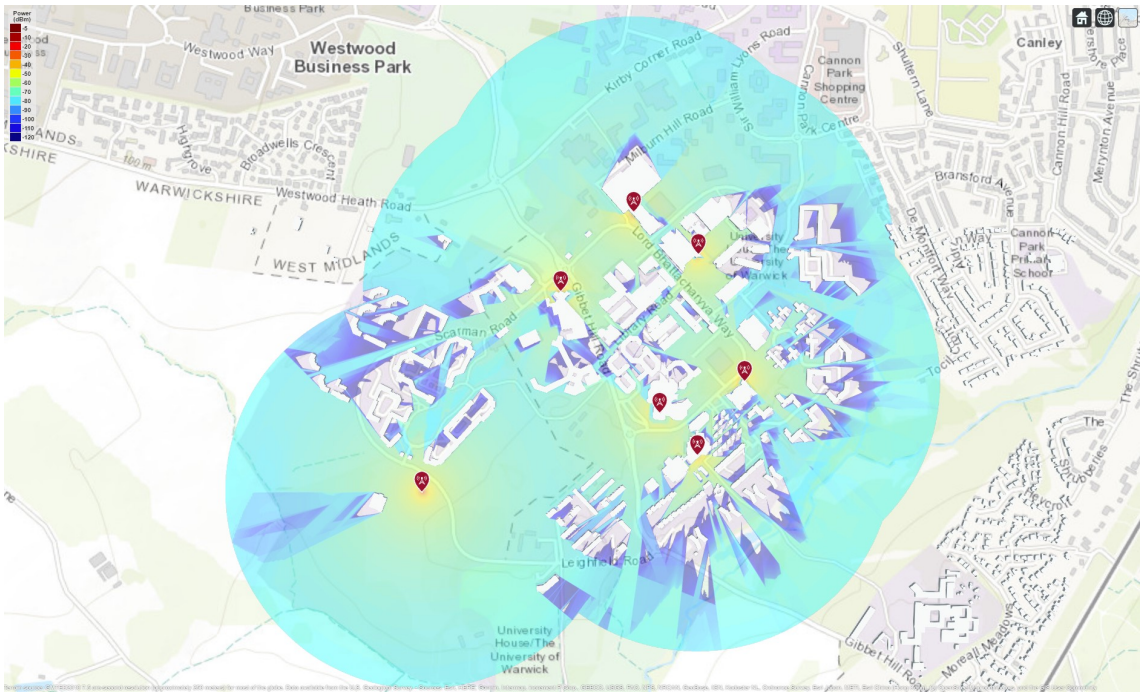

Figure 4.2: Coverage provided by all of the base stations on campus (excluding the Gibbet Hill campus), showing that the received power is around −50dBm close to the base stations and attenuates to approximately −80dBm around the edges of campus. This fading would continue if the radius of analysis was extended.

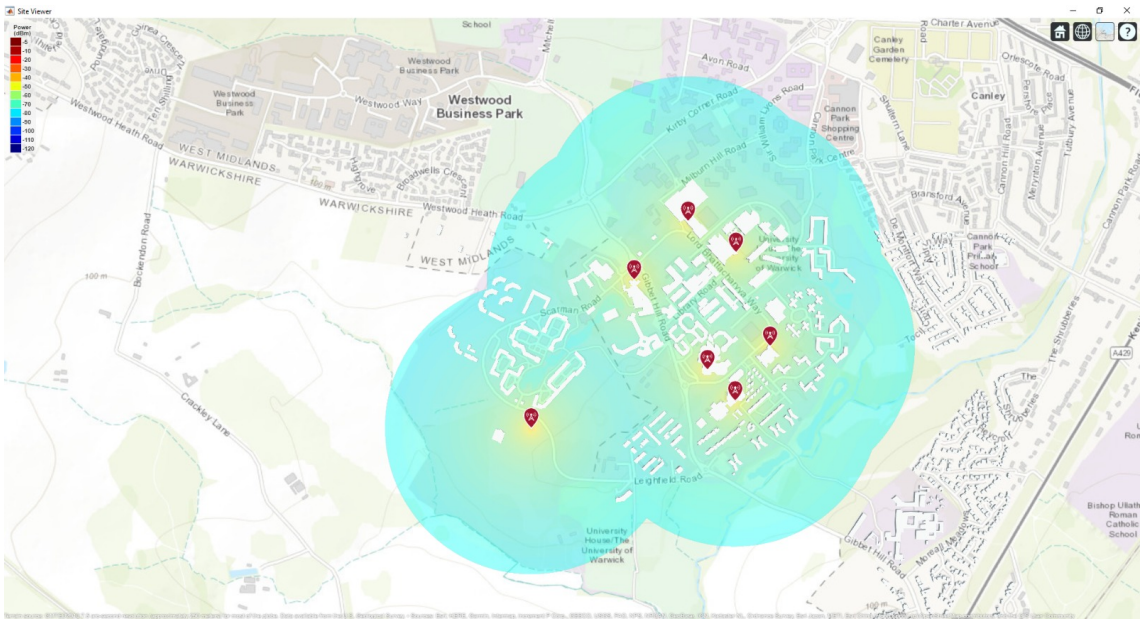

Figure 4.3: Free space model of the campus network, showing no shadowing and reduced attenuation compared to Figure 4.2. This model does not consider terrain or buildings, therefore assuming a direct LOS link for every communication link and no multi-path dispersion. The only factor contributing to the attenuation is the distance between the transmission and reception antennae.

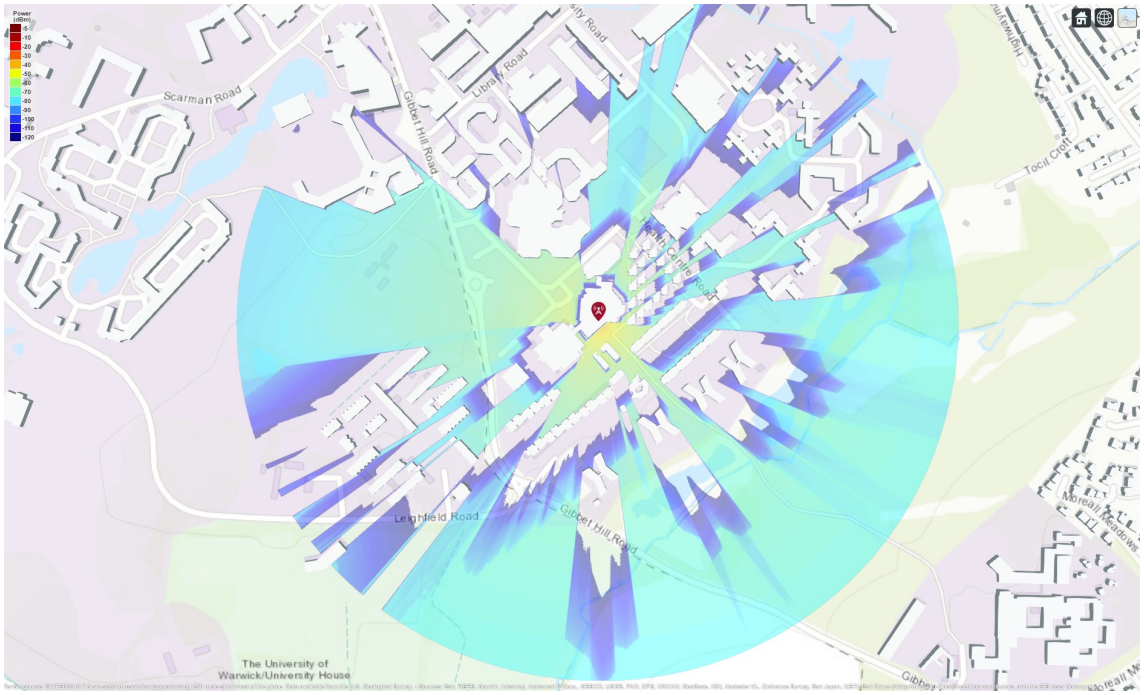

Figure 4.4: Zoomed in view of the coverage provided by the Student Union base station only. This shows the large effect that shadowing has on the received power from each individual base station, and is a visual representation of the coverage area and network strength that a drone replacement should replicate.

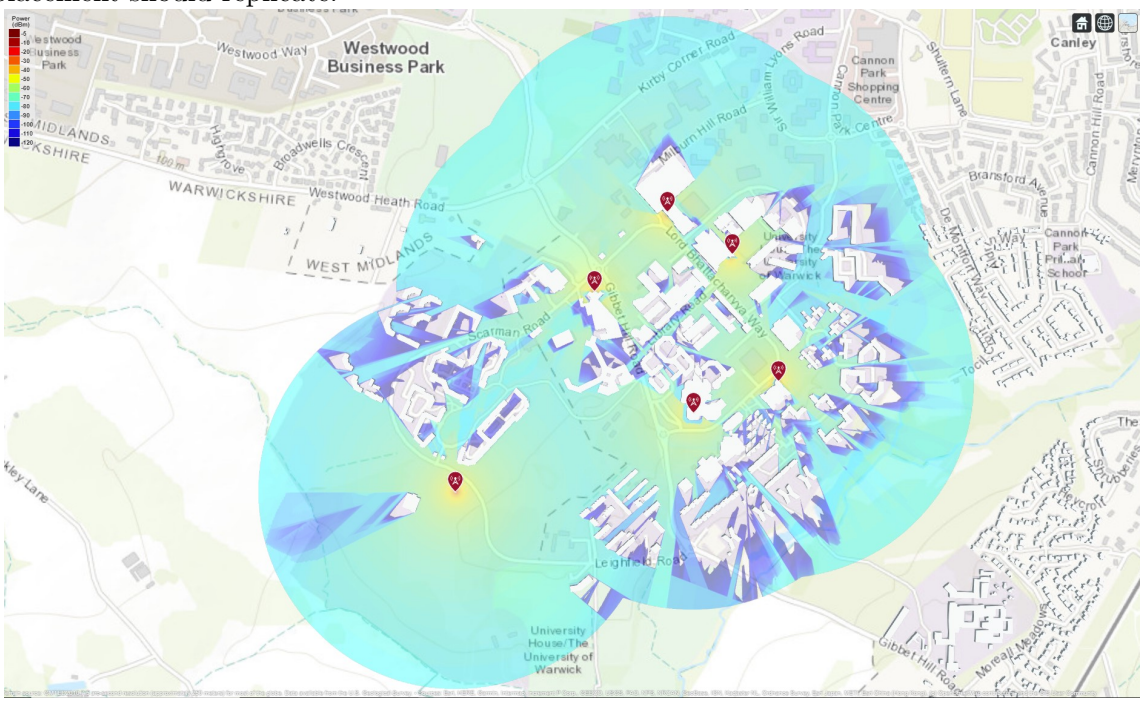

Figure 4.5: Visualisation of the campus network strength when the base station on top of the Student Union has failed. This could be due to a temporary error or a more serious case of equipment damage, such as the damage that infrastructure can suffer during natural disasters. Although subtle, an increase in the attenuation around the Rootes and Bluebell accommodations is noticeable in comparison to Figure 4.2, as is an increase in shadowing in the southeast sector of campus.

Figure 4.6: Coverage provided by a single drone replacement cell flying 2m above the coordinates of the Student Union base station. Compared to Figure 4.4, this shows a decrease in the overall received power (demonstrated by the darker shade of blue) but a simultaneous decrease in the effect of shadowing on the signal strength. The increased height of the transmission antennae mean that the building height is of less consequence than when the antennae is mounted on the building.

Figure 4.7: Full coverage heatmap when the drone replacement is implemented and integrated with the pre-existing campus infrastructure. The difference between this network simulation and the normal operating conditions shown in Figure 4.2 is small enough to be unnoticeable in this model, validating the use of a drone replacement and demonstrating that this is a valuable way to restore a communications network rapidly and effectively when the terrestrial infrastructure is damaged.

4.2 Graphs

4.2.1 Initial case - normal operating conditions

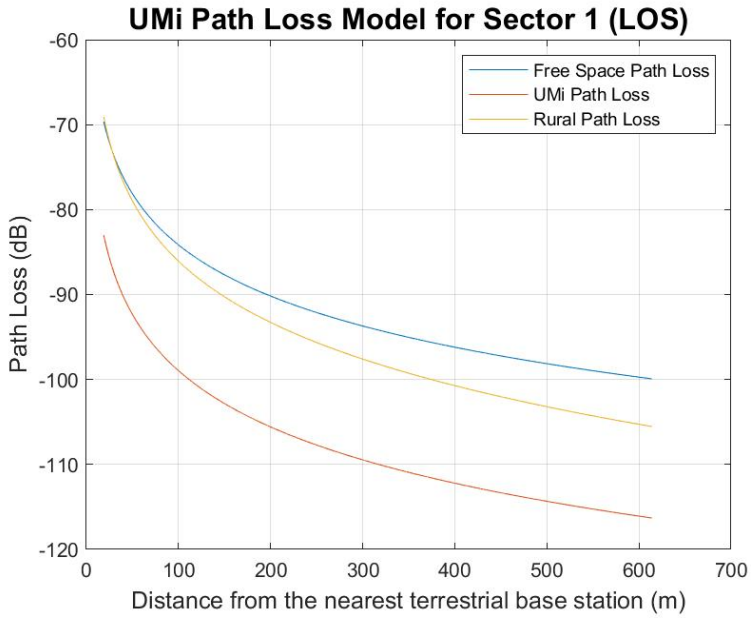

Figure 4.8: Path loss for Sector 1 under usual network conditions. The close correlation between the free space and rural path loss is expected, as under rural conditions there is less shadowing and multi-path dispersion causing attenuation. The higher attenuation (shown by a larger path loss magnitude) of the urban micro propagation scenario is also as expected, with far more causes for attenuation existing in urban environments.

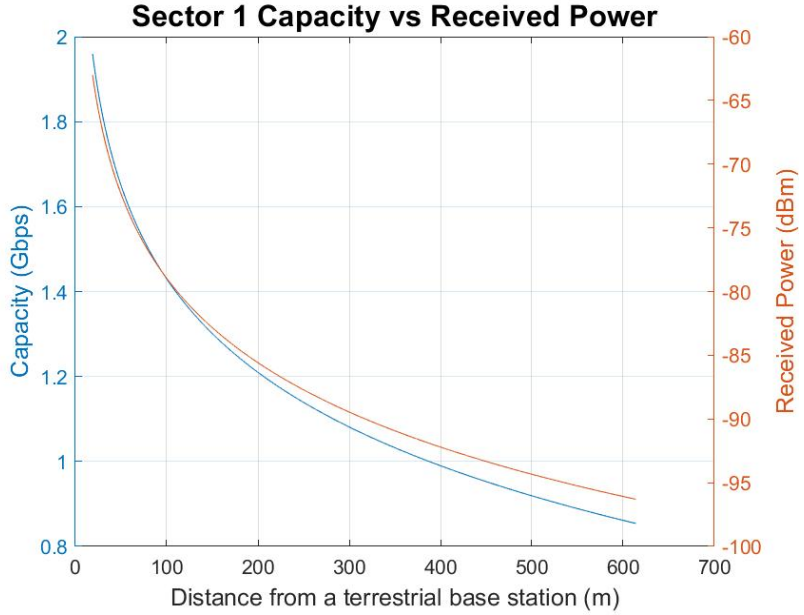

Figure 4.9: Received power and capacity for Sector 1 under normal operating conditions. The capacity shows a mid-range capacity of around 1.1Gbps, which is above the target value of 1Gbps mid-range capacity to allow multiple user high-definition video streaming. This is very positive as it suggests that the estimated values for transmitted power and AWGN are reasonable, and that the network can deliver the desired capacity.

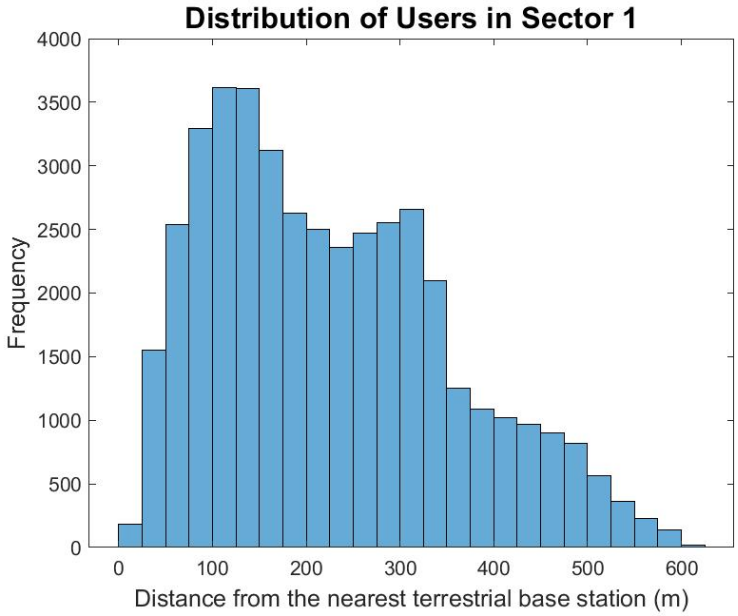

Figure 4.10: Histogram showing the user distribution in Sector 1 under initial conditions. This demonstrates that there is a significant positive skew to the distribution, with the majority of users falling before the mid-range value. This will lead to the majority of users in Sector 1 experiencing a capacity of above 1.1Gbps, above the target value for the model.

In Sectors 2 and 3, the propagation model was predicted to be suburban. A suburban model involves an assumption of a lower transmission height and buildings of three or fewer stories, rather than the 4 to 8 stories assumed in an urban environment. Furthermore, the suburban environment is predicted to have more foliage, obscuring the direct LOS links between transmission and reception antennae [43]. These factors combine to make the likelihood of a NLOS link higher in suburban environments. Suburban propagation environments tend to have lower path losses than urban environments over shorter distances, due to reduced dispersion caused by narrow streets and tall buildings, but over longer distances the increased foliage and decreased transmission height cause more significant attenuation.

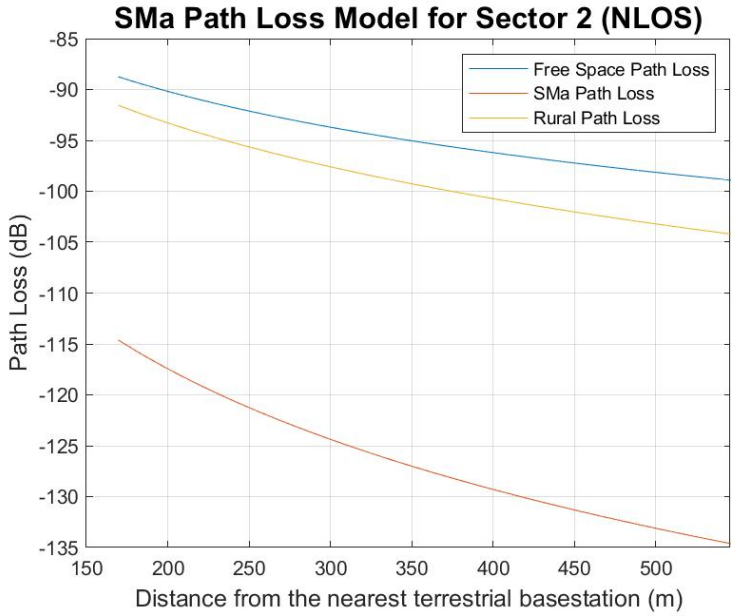

Figure 4.11: Path loss for Sector 2 under normal operating conditions. There are no base stations located directly within Sector 2, meaning that the rural and free space path losses do not demonstrate the convergence at lower distances seen in Figure 4.8 – however, they are still close enough together to validate the model. The significantly larger path loss experienced in a suburban propagation model is due to the NLOS propagation and increased multi-path dispersion and fading the signal will undergo.

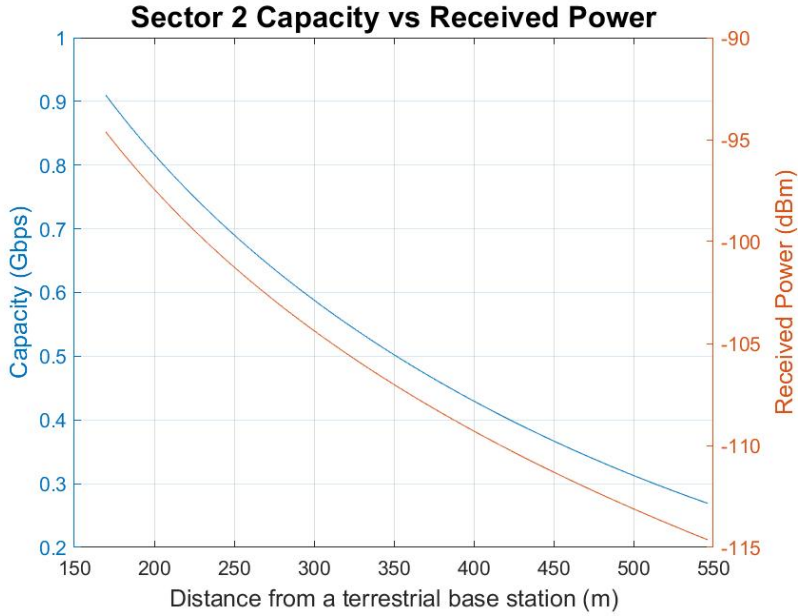

Figure 4.12: Received power and capacity in Sector 2 under normal operating conditions. Due to the distance of Sector 2 from any of the campus base stations, both capacity and received power are significantly lower than in both Sectors 1 and 3 throughout Sector 2. The mid-range capacity does not fall above the 1Gbps target value for streaming high-definition video to multiple users, suggesting that if this is required, a more powerful transmission signal should be used, or a transmission antenna placed locally.

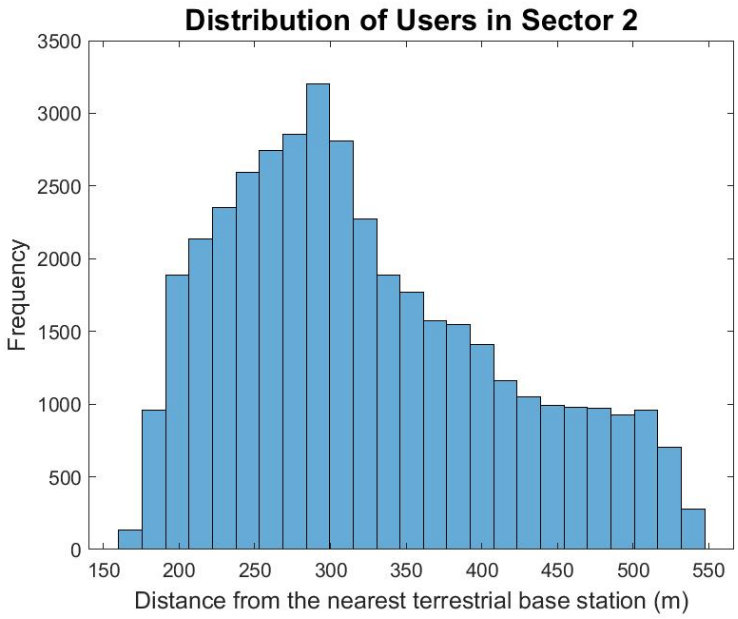

Figure 4.13: Histogram showing the user distribution in Sector 2 under initial conditions. As in Figure 4.10, there is a significant positive skew to the distribution, with the majority of users falling before the mid-range value. This will lead to the majority of users in Sector 1 experiencing a capacity of above 630Mbps.

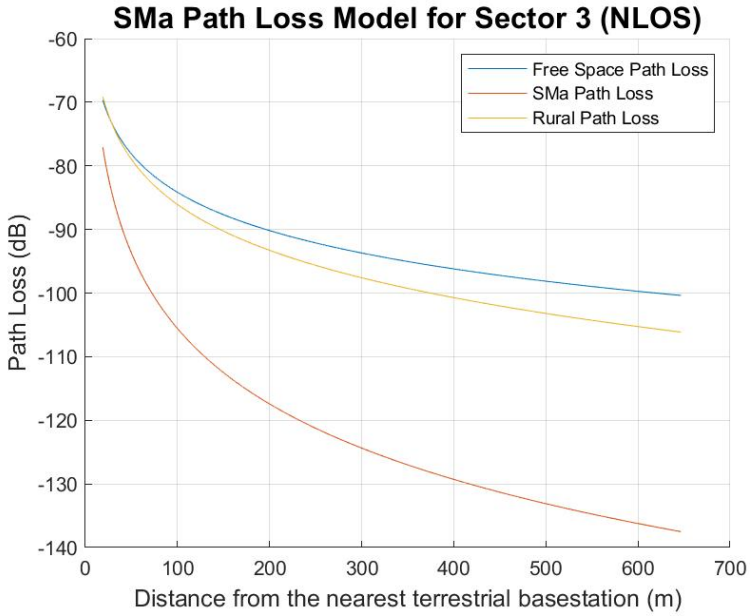

Figure 4.14: Path loss for Sector 3 under normal operating conditions, demonstrating again the similarity between the rural and free space path loss models, and the increased attenuation introduced in a suburban propagation environment. The increasing negative gradient of the suburban path loss line illustrates the heightened impact of distance on the suburban model compared to the other two.

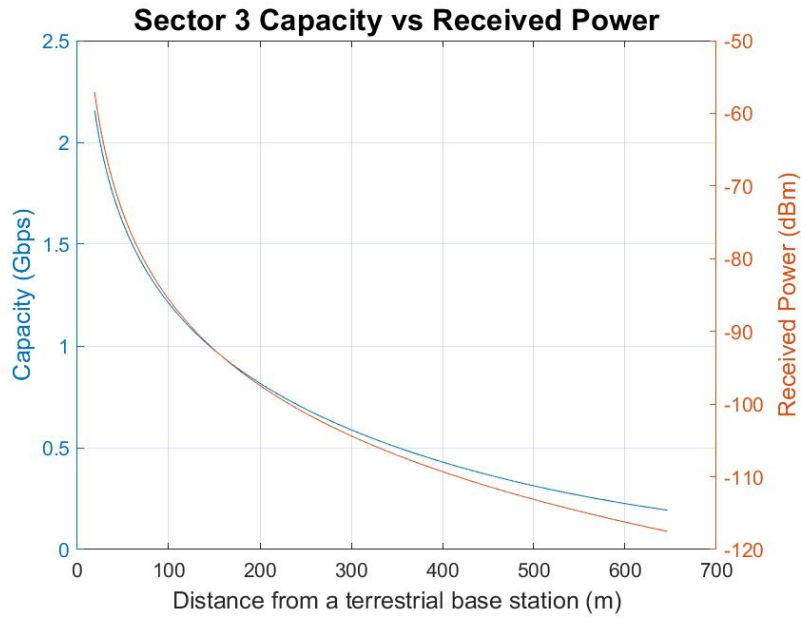

Figure 4.15: Received power and capacity in Sector 3 under normal operating conditions. Due to the lower path loss suburban propagation causes compared to urban propagation over short distances, the initial capacity is well within the target range. However, the increased attenuation over distance causes the capacity to fall out of the target range around 150m away from a base station.

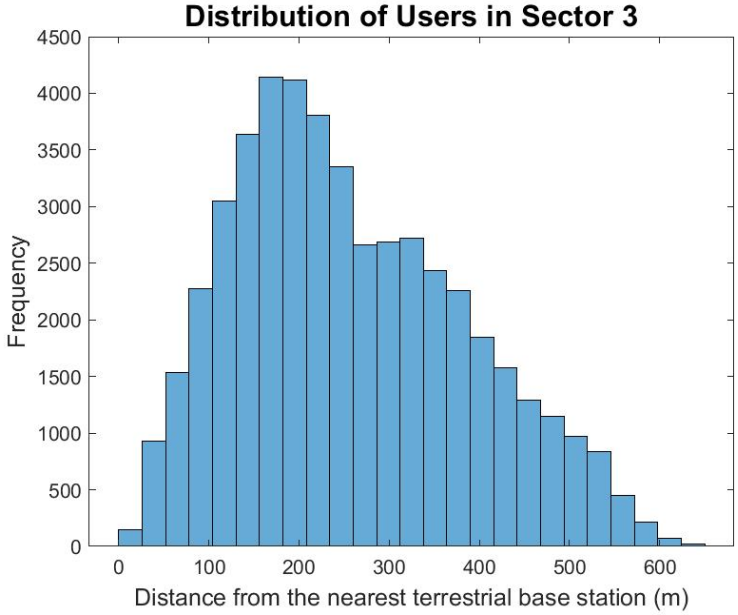

Figure 4.16: Histogram showing the user distribution in Sector 3 under initial conditions. The distribution of users here is closer to a normal (Gaussian) distribution than in Figures 4.10 and 4.13, bu the mode value is still well before the mid-range.

4.2.2 Failure case – when the Student Union base station is removed

Removing a base station from the model has no effect on the power and capacity graphs generated, as nothing about the propagation model changes and so the path loss for each scenario is the same as in **??**. This results in identical power and capacity plots. The difference comes in the distribution of the users. Without the Student's Union base station, more users are significantly further away from a base station than under initial conditions, leading to them experiencing lower capacity levels. Sector 3 is far enough away from the Student Union that an insignificant number of locations within the Sector would receive a signal from that base station, so hereon only Sectors 1 and 2 will be considered.

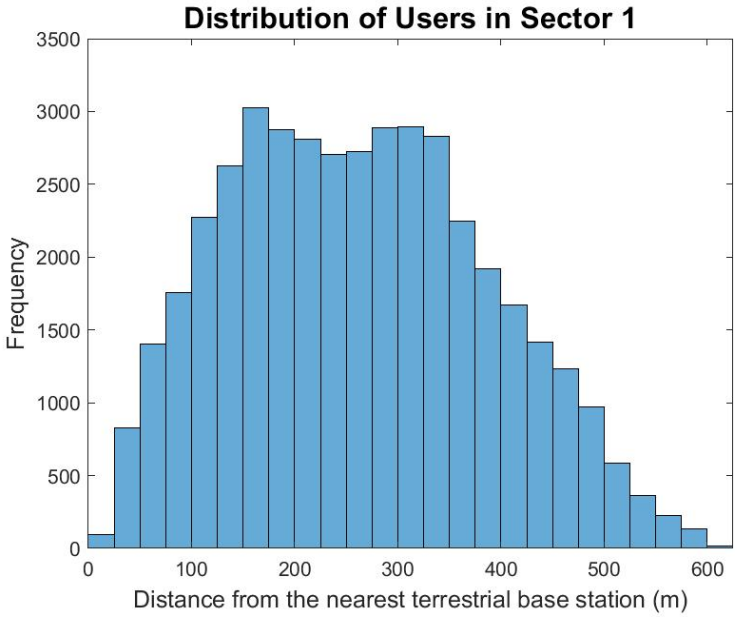

Figure 4.17: Histogram showing the user distribution in Sector 1 under failure conditions. This demonstrates that the positive skew of the distribution has been significantly reduced, meaning that more users are now further from a base station than they were when the Student Union base station was operational.

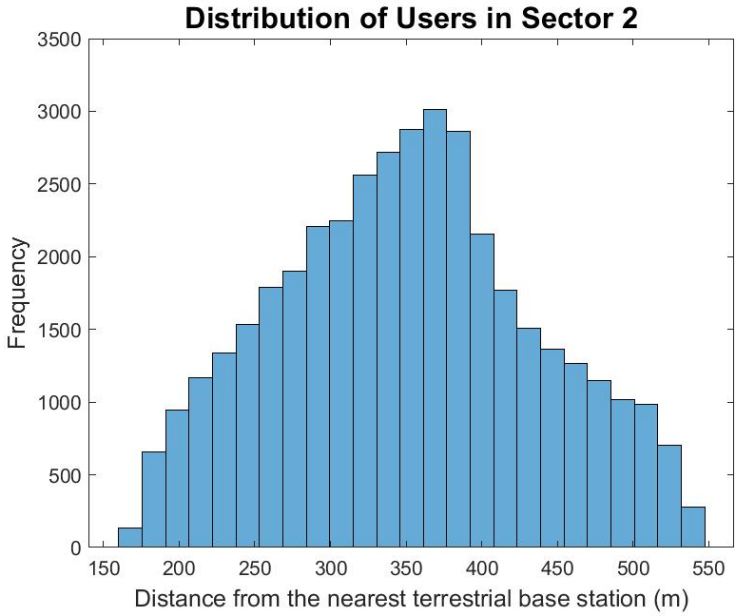

Figure 4.18: Histogram showing the user distribution in Sector 2 under failure conditions. This shows an almost normal (Gaussian) distribution, which is a significant change from the positive skew in Figure 4.13. As there are no base stations in the sector, and now an almost normal distribution is being followed, it is clear that many users in Sector 2 initially had the Student Union base station as their closest transmission antenna.

4.2.3 Drone case – when a drone cell is flown above the Student Union base station to restore capacity

In order to compare the drone replacement with the original terrestrial infrastructure, the following graphs plot the original path loss, received power, and capacity of the network, with the functioning terrestrial base station, against the path loss, received power and capacity of the network when the Student Union base station is replaced by a transmission antenna on a drone replacement, flying 2m above the original antenna and transmitting $1/10th$ of the original signal power. Only users who have the Student Union as their local base station are included, so the distribution of users throughout the distance array is even. The abbreviation TXS is used to refer to the terrestrial base station located at the Student Union.

In Sector 1, the additional height of the drone was considered to be sufficient to change the path loss propagation scenario from urban to suburban, as discussed in the Modelling chapter. In Sector 2, however, the increase in height did not lead to a change in the propagation scenario. This is both due to the NLOS conditions already accounting for many of the additional factors, and because the next 3GPP model is a free space model, which would be unacceptably optimistic due to its negligence of terrain and buildings.

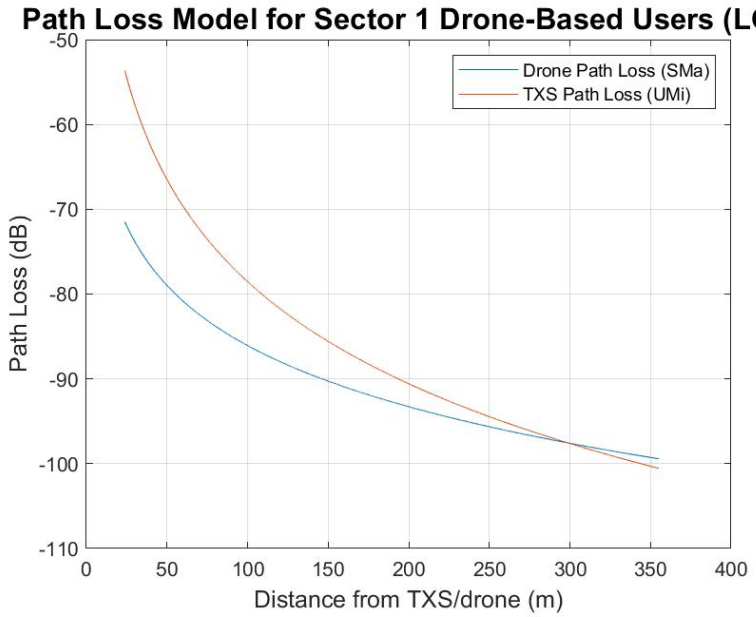

Figure 4.19: Path loss for Sector 1 users who are closest to the Student Union base station under both normal and drone-based operating conditions. The difference in propagation scenarios can be seen to change the shape of the path loss significantly, with the urban model having less path loss for users close to the base station but the suburban model resulting in less path loss for users more than 300m away. While a minority of users are at this distance from a base station on the University of Warwick campus, in other scenarios more users may be at this distance or further from their nearest base station.

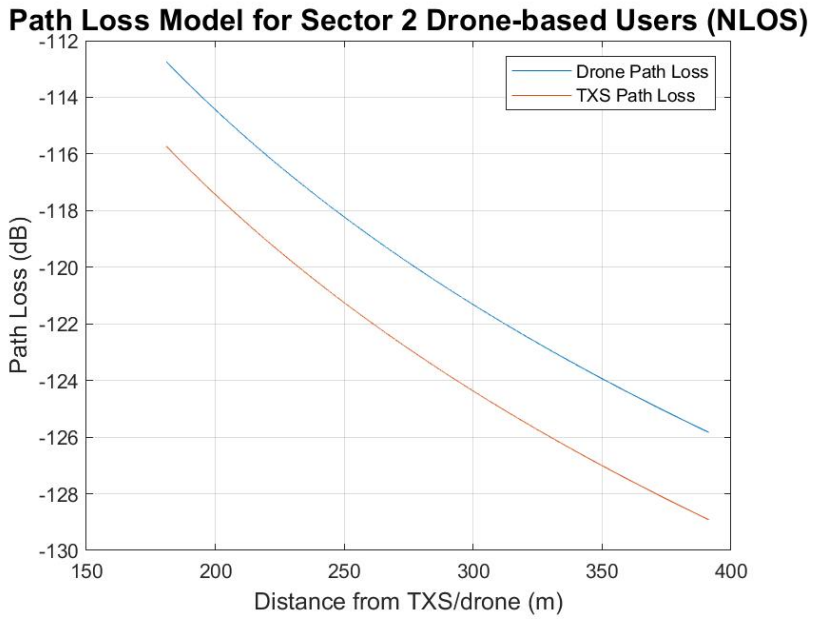

Figure 4.20: Path loss for Sector 2 users who are closest to the Student Union base station under both normal and drone-based operating conditions. As in this case, the propagation scenario does not change but is suburban for both the TXS and the drone cases, the relationship between the two is closer than in Sector 1. As path loss is a ratio rather than an absolute value, the fact that the drone experiences less path loss is expected, as the additional height of the transmission antenna will reduce the multi-path fading and scattering between the transmission and reception antennae.

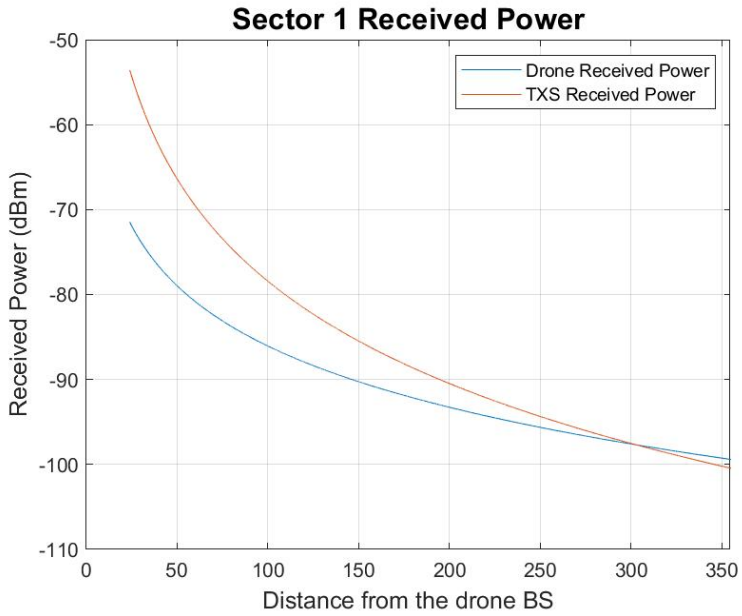

Figure 4.21: Received power for users in Sector 1 under normal and drone-based operating conditions. The relationship between the two scenarios is the same as in the Figure 4.19, with the urban model resulting in more received power at close distances and the suburban model overtaking around 300m from the base station. This is despite the difference in the transmission powers of the two scenarios.

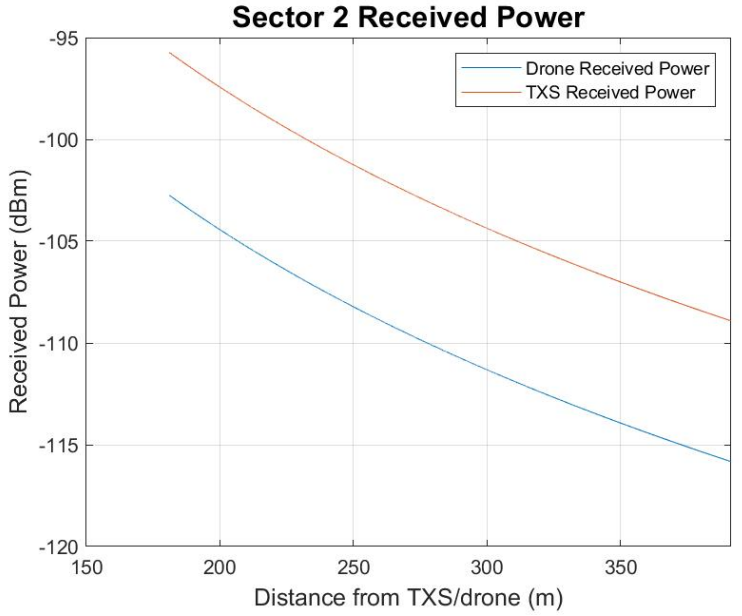

Figure 4.22: Received power for users in Sector 2 under normal and drone-based operating conditions. The received power is around 7dBm lower for the drone-based scenario than under normal operating conditions, which is a small but significantly difference amounting to around 5mW.

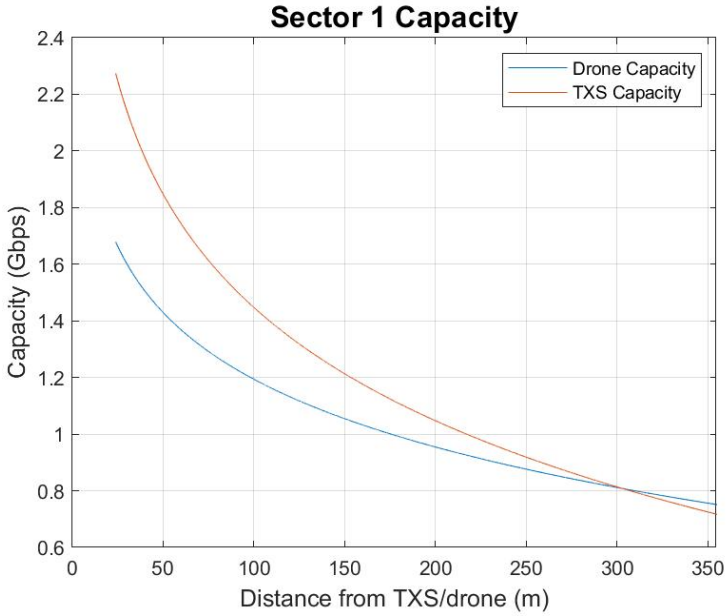

Figure 4.23: Capacity for users in Sector 1 under normal and drone-based operating conditions. This demonstrates the validity of a drone-based solution to a terrestrial base station outage, as the capacity is largely (although not wholly) restored by the drone replacement antenna. Capacity is within the suggested range up to a distance of approximately 175m from the transmission antenna.

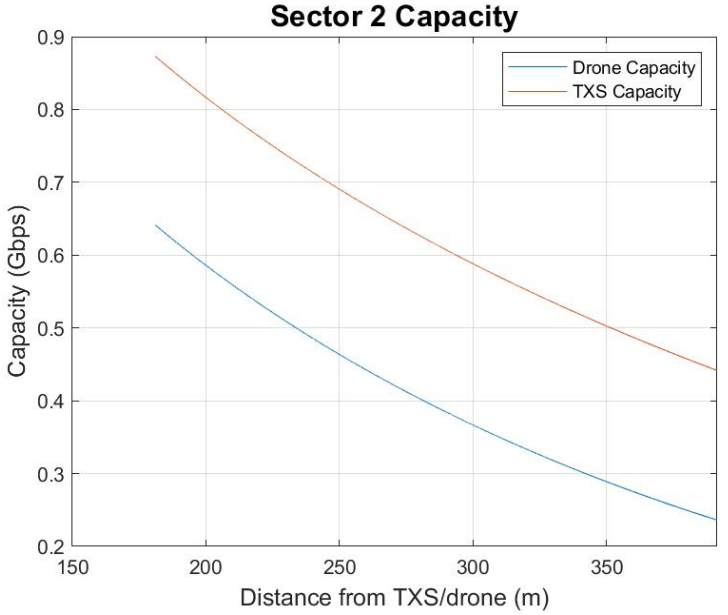

Figure 4.24: Capacity for users in Sector 2 under normal and drone-based operating conditions. The difference in the TXS capacity between this model and Figure 4.12 is unexpected, as the two should be the same. However, the range is similar, and demonstrates that while there is a considerable amount of attenuation in the drone-based solution, it remains above 200Mbps throughout the range.

5 Analysis

5.1 Initial Case Analysis

The heatmap generated to visualise the coverage across campus under normal conditions (Figure 4.2) shows that the average power received is around -75dBm. Modern mobile phones generally have signal when the received signal power is above -110dBm, and received signal strengths typically range between -50dBm and -110dBm. Although practical measurements of the signal strength on the University of Warwick campus were not taken to verify this model, the range seems reasonable and in line with anecdotal evidence. The large difference between the heatmaps in Figures 4.2 and 4.3 show the over-simplification that hampers a free space model in analysing a communications network in built up areas. The terrain and buildings clearly have a huge impact on the received signal strength. This invites questions about the accuracy of the empirical models used in the MATLAB modelling, as the deterministic modelling done to generate these heatmaps utilised a specific terrain map. However, it can be seen that the MATLAB results are largely in the same range as the heatmaps suggest they should be, and the justifications for using empirical models (discussed in Chapter 2) stand. Terrain maps are not always available and generating these heatmaps took significantly longer than running the empirical analysis.

Figure 4.4 shows the large shadowing caused by each individual base station. As the transmission antennae are mounted on the buildings, it is unsurprising that the signal is hugely affected. The heatmaps generated use the Longley-Rice Propagation Model, which accounts for scattering and dispersion. The height of the transmission antennae is a very influential factor in how much attenuation signals undergo in urban environments, where scattering plays an essential role in propagation as LOS links are less likely. This is accounted for in the empirical models for Sector 1 by having the building-mounted transmission antennae assume an UMi propagation path, and the higher, drone-mounted transmission antennae assume a SMa path. The effect of having several base stations in a small built-up area is therefore obvious, reducing shadowing by increasing the number of angles at which the signal is transmitted down into the area. In rural regions, this shadowing is less of an issue, as there are fewer buildings to attenuate the signal. This may lead to a single base station being sufficient to serve a much larger radius.

Figures 4.8, 4.11, and 4.14 all demonstrate the anticipated close correlation between the rural and free space path loss models. The most significant factor differentiating the two is, again, the height of the transmission antennae and the average building height, returning to the previous assertion than multi-path dispersion and scattering are key factors to reduce in order to improve signal strength. The greater the difference in height between the transmission antennae and the average building height, the less shadowing the buildings will cause. Obviously, there

will come a point where the increased height of the transmission antennae leads to the path becoming long enough that this trade off is inadvisable, but this point is significantly higher than the altitude at which any drone would fly. The path loss models in Figures 4.8, 4.11, and 4.14 have reasonable ranges and the expected shapes, suggesting that the assumptions and approximations made for using the empirical model were reasonable. To improve the accuracy of these models, measurements of these variables could be taken, although this was out of scope for this project.

Figure 4.11 demonstrates that there is no base station located in Sector 2 of campus, as the shortest distance between a potential user and a base station is over 150m. This causes all Sector 2 graphs to demonstrate a far smaller segment of the path loss behaviour than Sectors 1 and 3, meaning that the path loss curves are less visible. The higher path loss shown in Sector 2 is also expected, both due to the increased path length between the transmission and reception antennae and the NLOS path.

The mid-range capacities for the three sectors are 1.1Gbps, 630Mbps, and 600Mbps respectively. At no point in range do any of the sectors fall below 200Mbps, which as previously discussed is the very upper end of the capacity delivered by current market leaders in temporary communication network solutions. Sector 1, the only UMi environment modelled, performs particularly strongly, with the capacity not falling below the accepted value of 800Mbps in range. Figures 4.10 and 4.13 show that in Sectors 1 and 2, the distribution of users is positively skewed, meaning the majority of people will experience capacity above the mid-range, while in Sector 3, Figure 4.16 shows a distribution closer to normal but where the mode is still well before the mid-range. This makes these modelled results very promising.

5.2 Failure Case Analysis

Figure 4.5 shows an increase in the attenuation around Rootes and Bluebell accommodations when the Student Union base station fails. The benefits of having many transmission antennae in an urban environment is clear, as the removal of only one from the model has caused the shadowing effect to be noticeably stronger than in Figure 4.2.

The MATLAB graphs analysing the path loss, received power, and coverage under failure conditions are identical to the graphs in the previous section. This is because they do not reflect the different distances of people from base stations. Nothing about the propagation scenario has changed, so path loss in each sector is the same. This means capacity and received power at a certain distance from a base station will still be the same – it is just the location of the users that is different. This is demonstrated in Figures 4.17 and 4.18, which when compared to Figures

4.10 and 4.13 show that the skew of the distribution is more heavily weighted towards being further from a base station than in the initial case. This is because people will now receive signal from a different base station. Illustratively, in the initial case, 34.5% of the users generated in Sector 1 and 35.5% of users in Sector 2 were closest to the Student Union base station, and all of these users will be at a significantly longer distance from a base station under the failure conditions. Figures 4.17 and 4.18 show that under failure conditions, most users are around $300 - 450$m from a base station, with the strong positive skew the distributions exhibited under normal operating conditions being considerably reduced.

5.3 Drone Replacement Analysis

The coverage map for the drone-based solution (Figure 4.7) is almost indistinguishable from the initial coverage heatmap showing normal working conditions (Figure 4.2). Compared to the terrestrial base station, the drone-mounted antenna demonstrates decreased received power but also decreased shadowing. The change of propagation scenarios utilised in Sector 1 changes the shape of the path loss model as shown in Figure 4.19, thus affecting both the received power and the capacity graphs (Figures 4.21 and 4.23, respectively). The urban modelling results in less path loss at short distances but more at longer distances, while there is a shallower attenuation gradient in the suburban path loss, which starts at a greater value but becomes less than the urban path loss at distances over 300m. In Sector 2, Figure 4.20 shows lower path loss in the drone. This is caused by the higher altitude of the transmission antenna, reducing shadowing. The linear relationship between the two path loss models demonstrates that the dependence of path loss on transmission antenna height is linear. The difference in the two path loss models remains at around 4dB for all users, showing that the drone solution improves on the path loss by elevating the transmission antenna.

Figure 4.23 shows that the capacity delivered by the drone in Sector 1 drops below the target capacity of 1Gbps at paths over 275m, and below the accepted capacity of 800Mbps at around 310m. In Sector 2, Figure 4.24 shows capacity is under 1Gbps at all distances, which was expected, as this was also the case under normal operating conditions due to the increased distances from base stations and the NLOS propagation model. However, the capacity remains above 500Mbps until path distances of above 230m, and it is notable that it does not drop below 200Mbps within range. Throughout Sector 2, the received power (Figure 4.22) is 7dBm lower from the drone than from the transmission station. This maps to a difference of around 5mW, which is very small considering the drone transmission power is an order of magnitude below the terrestrial base station transmission power, emphasising again the impact that the height of

the transmission antenna has on the path loss experienced.

5.4 Analysis Conclusion

Sector	**Mid-range Capacity** (Gbps)	**Status**
1	1.1	Above Target
2	0.63	Successful
3	0.60	Successful

Table 3: Summary of results for drone-based solution

The results presented by this modelling are summarised in Table 3. Status is listed 'Above Target' where the modelled capacity exceeds the initial target value of 1Gbps, 'Successful' where it remains within the accepted range of $200 - 800$Mbps, and 'Failure' otherwise. The target capacity set in this project of 1Mbps is very high compared to the current market standard in temporary communications network capacity, and as the model of the network operating under normal conditions does not meet this target in two of the three sectors, it makes more sense to determine success or failure of the drone based results with regards to the current market-leading standard of 200Mbps, which is large enough to stream $4K$ video with a latency equivalent to terrestrial network speed [18]. Under these criteria, this modelling is very successful, with all three cases resulting in a mid-range capacity within the desired range. This suggests that a drone-mounted antenna would be capable of restoring capacity to a high level should a base station fail. Therefore, this work presents a strong case for the further exploration of using drone-mounted antennae to restore communications networks temporarily.

6 Conclusions

This work has demonstrated that emergency network coverage can be provided to a high standard through the deployment of drone-mounted transmission antennae. Through modelling the University of Warwick campus network under normal conditions and when a base station is simulated to have failed and been replaced with a drone, it has been shown that relatively minor attenuation occurs using temporary drone-based infrastructure. Therefore, this is a promising and valuable avenue for research, with wide-ranging potential applications in humanitarian aid and disaster relief, where the ability to communicate seamlessly is of vital importance yet where network infrastructure is often critically damaged.

As this research has produced results that are both original and specific to a small geographical location (the University of Warwick campus), this report could form the foundation of a use case analysis for resilient 5G networks, to be presented at a conference for UK-based mobile network operators. While attenuation was observed between the terrestrial and drone-based infrastructure, the drone-based solution had significantly better modelled results than the current market leaders in temporary communications networks, providing over 200Mbps capacity in all scenarios and often considerably more. This makes this research highly relevant to the mobile network industry, especially as 5G becomes the standard for mobile networks across the country.

HAPs will present a compelling alternative to this approach when the technology is mature, but they are still not functional as a replacement for terrestrial infrastructure. Disaster scenarios are happening with greater frequency every year. This is not a problem that can wait for an optimal solution. The work presented here shows strong potential for being an improvement on the lacklustre current methods, as well as utilising mature technologies which can be deployed as a practical solution with ease, allowing for fast development. Differences between the modelled results and any future practical results are likely to be due to a drone that is not perfectly stationary, and to the path loss models being governed by approximated factors. Therefore, testing this solution through practical experimentation should be a research priority. Measurements of received power should be taken in order to derive an experimental path loss and compare it to the theoretical, with the goal of actually establishing a network with temporary infrastructure. Extensions on the theoretical work presented here should focus on multi-drone scenarios covering a wider landmass than the University of Warwick campus. Future research in this area should pursue the use of drone-based methods to restore communications network coverage in the event of ground infrastructure being temporarily unavailable as a priority, due to its huge promise and potentially life-saving impact it will have.

References

[1] 3GPP, "3GPP Technical Report 36.814 V9.0.0 (2010-03)," Valbonne, France, Tech. Rep., 2010.

[2] BBC News Asia, "Tonga volcano: Internet restored five weeks after eruption," Available at https://www.bbc.co.uk/news/world-asia-60458303 (22/02/2022).

[3] K. Duffy, "SpaceX's Starlink starts work restoring internet access to volcano-hit Tonga after Elon Musk offered to help," Available at https://www.businessinsider.com/elon-musk-spacex-tonga-restore-internet-starlink-volcanic-eruption-cable-2022-2?r=USIR=T (07/03/2022).

[4] H. Toya and M. Skidmore, "Information/communication technology and natural disaster vulnerability," *Economics Letters*, vol. 137, no. 9, pp. 143–145, 2015.

[5] ——, "Cellular Telephones and Natural Disaster Vulnerability," *Sustainability*, vol. 10, no. 9, p. 2960, 2018.

[6] A. Mauthe, D. Hutchison, E. Cetinkaya *et al.*, "Disaster-resilient communication networks: Principles and best practices," Halmstad, Sweden, 2016.

[7] National Commission on Terrorist Attacks Upon the United States, "The 9/11 Report: Final report of the National Commission on Terrorist Attacks Upon the United States (Authorized Edition)," 2004.

[8] Cabinet Office, "Keeping the Country Running: Natural Hazards and Infrastructure," 2011.

[9] C. Stokel-Walker, "Tonga's volcano blast cut it off from the world. Here's what it will take to get it reconnected," *MIT Technology Review*, 2022.

[10] Excelerate, "Vehicle Mounted Satellite Communications," Available at https://www.excelerate-group.com/vehicle-mounted-satellite-communications/ (27/07/2021).

[11] Verizon Frontline News Centre, "Verizon Frontline unveils THOR: mobile, 5G rapid-response command center," Available at https://www.verizon.com/about/news/verizon-frontline-unveils-thor (07/07/2021).

[12] A. Saif, N. Kaharundin, and K. Ariffin, "Unmanned Aerial Vehicles for Post-Disaster Communication Networks," Shah Alam, Malaysia, 2020.

[13] Y. Chen, H. Zhang, and Y. Hu, "Optimal Power and Bandwidth Allocation for Multiuser Video Streaming in UAV Relay Networks," *IEEE Transactions on Vehicular Technology*, vol. 69, no. 6, pp. 6644–6655, 2020.

[14] C. Zhan, H. Hu, L. Xiufeng *et al.*, "Joint Resource Allocation and 3D Aerial Trajectory Design for Video Streaming in UAV Communication Systems," *IEEE Transactions on Circuits and Systems for Video Technology*, vol. 31, no. 8, pp. 3227–3241, 2021.

[15] Z. Yao, W. Cheng, W. Zhang, and H. Zhang, "Resource Allocation for 5G-UAV-Based Emergency Wireless Communications," *IEEE Journal on Selected Areas in Communications*, vol. 39, no. 11, pp. 3395–3410, 2021.

[16] H. Niu, X. Zhao, and J. Li, "3D Location and Resource Allocation Optimization for UAV-Enabled Emergency Networks Under Statistical QoS Constraint," *IEEE Access*, vol. 9, pp. 41 566–41 576, 2021.

[17] D. Grace and M. Mohorcic, *Broadband Communications via High Altitude Platforms*. Chichester, UK: John Wiley & Sons, 2011.

[18] Stratospheric Platforms Ltd, "SPL Announces World First 5G Transmission From The Stratosphere," Available at https://www.stratosphericplatforms.com/news/world-first-5g-transmission/ (03/03/2022).

[19] S. AlGhamdi, "World-First Trial of 5G HAPS Technology Takes Place in Saudi Arabia In the Red Sea Project," Riyadh, Saudi Arabia, 2022.

[20] M. Mollel and M. Kisangiri, "Comparison of Empirical Propagation Path Loss Models for Mobile Communnication," *Computer Engineering and Intelligent Systems*, vol. 5, no. 9, 2014.

[21] R. Ghanem and A. Doostan, "On the construction and analysis of stochastic models: Characterisation and propagation of the errors associated with limited data," *Journal of Computational Physics*, vol. 217, no. 217,

pp. 63–81, 2006.

[22] M. Higgins, *MSc Link Budget and Channel*, ser. Lecture Notes. Coventry, UK: Warwick Manufacturing Group, 2021.

[23] N. Nkordeh, A. Atayero, F. Idachaba, and O. Oni, "LTE Network Planning using the Hata-Okumura and the COST-231 Hata Pathloss Models," *Covenant University Repository*, 2014.

[24] T. Thomas, M. Ryabakowski, S. Sun *et al.*, "A Prediction Study of Path Loss Models from 2-73.5 GHz in an Urban-Macro Environment," *IEEE 83rd Vehicular Technology Conference (VTC Spring)*, 2016.

[25] G. MacCartney, J. Zhang, S. Nie, and T. Rappaport, "Path loss models for 5G millimeter wave propagation channels in urban microcells," *IEEE Global Communications Conference (GLOBECOM)*, 2013.

[26] Q. Feng, E. Tameh, A. Nix, and J. McGeehan, "Modelling the Likelihood of Line-of-Sight for Air-to-Ground Radio Propagation in Urban Environments," *IEEE Global Communications Conference (GLOBECOM)*, 2006.

[27] Q. Feng, J. McGeehan, E. Tameh, and A. Nix, "Path Loss Models for Air-to-Ground Radio Channels in Urban Environments," *IEEE 63rd Vehicular Technology Conference*, 2006.

[28] M. Mozaffari, W. Saad, M. Bennis, and M. Debbah, "Efficient Deployment of Multiple Unmanned Aerial Vehicles for Optimal Wireless Coverage," *IEEE Communications Letters*, pp. 1647–1650, 2016.

[29] F. Almalki and M. Angelides, "Deployment of an aerial platform system for rapid restoration of communications links after a disaster: a machine learning approach," *Computing*, vol. 102, pp. 829–864, 2020.

[30] H. Spanner, "Is 5G really a threat to airlines?" Available at https://www.sciencefocus.com/news/is-5g-really-a-threat-to-airlines/ (21/01/2022).

[31] Federal Communications Commission (FCC), "In the Matter of Expanding Flexible Use in the 3.7-4.2 GHz Band, GN Docket No. 18-122," Washington DC, USA, 2020.

[32] ——, "Expanding Flexible Use in Mid-Band Spectrum Between 3.7 and 24 GHz," Washington DC, USA, 2017.

[33] 5G Americas, "Mid-band Spectrum and the Coexistence with Radio Altimeters," 2021.

[34] Radio Technical Commission for Aeronautics (RTCA), "Assessment of C-Band Mobile Telecommunications Interference Impact on Low Range Radar Altimeter Operations," Washington DC, USA, 2020.

[35] Federal Aviation Authority (FAA), "FAA Statements on 5G," Washington DC, USA, 2022.

[36] D. Ramsey and J. Rogerson, "5G Frequencies in the UK," Available at https://5g.co.uk/guides/5g-frequencies-in-the-uk-what-you-need-to-know/ (15/01/2022).

[37] D. Tse and P. Viswanath, *Fundamentals of Wireless Communication*. Cambridge, UK: Cambridge University Press, 2004.

[38] Starlink, "High-Speed, Low Latency," Available at https://www.starlink.com/ (07/03/2022).

[39] MIT OpenCourseWare, *Introduction to EECS II: Digital Communication Systems*, ser. Lecture Notes. Boston, USA: MIT, 2014.

[40] H Kim, *Wireless Communications Systems Design*. Chichester, UK: John Wiley & Sons, 2015.

[41] K. Chamberlin and R. Luebbers, "An evaluation of Longely-Rice and GTD propagation models," *IEEE Transactions on Antennas and Propagation*, vol. 30, no. 6, pp. 1093–1098, 1982.

[42] P. I. Lazaridis, S. Kasampalis, Z. Zaharis *et al.*, "Longley-Rice model precision in case of multiple diffracting obstacles," Gran Canaria, Spain, 2015.

[43] T. Thomas, M. Rybakowski, and P. Krysiak, "Preliminary 5G Suburban Micro (SMi) Channel Model for Different Foliage Conditions," Washington DC, USA, 2016.